Clin. Lab. 2026;72:XXX-XXX

ORIGINAL ARTICLE

Shenfu Injection Alleviates Pancreatitis-Induced Damage and Oxidative Stress by Upregulating CLDN4 to Protect Endothelial Cells

Liming Xu, Chenghang Jiang, Tianpeng Wang, Shengang Zhou, Gaoxiang Li, Yueliang Zheng

Emergency and Critical Care Center, Department of Emergency Medicine, Zhejiang Provincial People's Hospital, Affiliated People's Hospital, Hangzhou Medical College, Hangzhou, Zhejiang, China

SUMMARY

Background: **Endothelial dysfunction represents a critical pathological feature of acute pancreatitis (AP). Shenfu injection (SFI) has been demonstrated to protect both endothelial cells and pancreatic tissues affected by AP; however, the precise mechanisms underlying its protective effects remain incompletely understood. The study investigated the protective role of SFI in oxidative-stressed endothelial cells and in acute pancreatitis through the regulation of CLDN4.**

Methods: **Human umbilical vein endothelial cells (HUVECs) were treated with oxidized low-density lipoprotein (ox-LDL) to create an oxidative stress environment, followed by SFI treatment to assess cell viability, apoptosis, and reactive oxygen species (ROS) levels. Additionally, shRNA technology was employed to knock down CLDN4 expression in order to evaluate its role in SFI-mediated protection. Finally, an AP rat model was established to investigate the effects of SFI on AP-induced pancreatic damage and the role of CLDN4.**

Results: **SFI significantly enhances cell viability, reduces apoptosis, and lowers ROS levels in HUVECs under oxidative stress. At the molecular level, SFI upregulates CLDN4 expression, and depletion of CLDN4 attenuates the protective effects of SFI against oxidative stress. In the AP rat model, SFI administration alleviated pancreatic tissue damage and reduced inflammation, while CLDN4 knockdown diminished these protective effects.**

Conclusions: **These findings identify CLDN4 as a key mediator of SFI's protective effects on both oxidative-stressed endothelial cells and inflamed pancreatic tissues, underscoring its potential as a therapeutic target in AP.**
(Clin. Lab. 2026;72:xx-xx. DOI: 10.7754/Clin.Lab.2025.250673)

Correspondence:
Chenghang Jiang
Emergency and Critical Care Center
Department of Emergency Medicine
Zhejiang Provincial People's Hospital
Affiliated People's Hospital
Hangzhou Medical College
No. 158 Shangtang Road, Gongshu District
Hangzhou, 310014, Zhejiang
China
Phone: +86 18814808488
Fax: +86 057185893799
Email: jiangchenghang@hmc.edu.cn

Manuscript accepted July 25, 2025

KEYWORDS

acute pancreatitis, endothelial dysfunction, Shenfu injection, oxidative stress, CLDN4

LIST OF ABBREVIATIONS

HUVECs - Human umbilical vein endothelial cells
AP - Acute pancreatitis
ROS - Reactive oxygen species
SFI - Shenfu injection
Ox-LDL - Oxidized low-density lipoprotein
TCM - Traditional Chinese medicine
SOD - Superoxide dismutase
NO - Nitric oxide
IHC - Immunohistochemistry
ELISA - Enzyme-linked immunosorbent assay

INTRODUCTION

The pathological events in acute pancreatitis (AP) encompass an intricate series of processes that result in pancreatic inflammation and autodigestion. These processes entail the infiltration of immune cells, premature activation of digestive enzymes, excessive release of inflammatory cytokines, and heightened vascular permeability, among others [3]. If left untreated, AP can worsen, triggering a systemic inflammatory response and multiorgan dysfunction, which may culminate in a life-threatening condition [4,5].

Endothelial cells form the specialized lining of blood vessels and lymphatic vessels, acting as a protective barrier between the circulating blood or lymph and surrounding tissues. These cells play a crucial role in maintaining essential physiological processes vital for vascular health [6,7]. Dysfunction of endothelial cells is associated with various conditions, including cardiovascular diseases, diabetes mellitus, and AP [8-10]. Hence, enhancing the function of endothelial cells could provide therapeutic benefits for treating these diseases.

Shenfu injection (SFI) is a traditional Chinese medicine (TCM) widely employed in the treatment of various diseases. It comprises ginsenosides and aconite alkaloids, which have demonstrated therapeutic efficacy in addressing cardiovascular diseases, ischemia-reperfusion injury, and AP [11-13]. At the molecular level, SFI is believed to enhance the functionality of vascular cells by activating the PI3K/Akt pathway, thereby boosting eNOS activity [14]. Nevertheless, the exact mechanism through which SFI safeguards endothelial cells remains inadequately understood.

Given the critical importance of endothelial dysfunction in AP and the extensively documented protective effects of SFI on endothelial cells, it is hypothesized that SFI may alleviate AP symptoms by enhancing endothelial cell function. To test this hypothesis, the impact of SFI on the viability, apoptosis, and ROS levels of ox-LDL-treated HUVECs was assessed. Subsequently, the role of CLDN4 in mediating the beneficial effects of SFI on oxidative-stressed HUVECs was investigated. Furthermore, we investigated the effect of SFI on the pancreatic tissue in an AP rat model and evaluated the impact of SFI on CLDN4-deficient inflammatory pancreatic tissues.

MATERIALS AND METHODS

Cell culture, ox-LDL, and Shenfu injection (SFI) treatment

HUVECs were obtained from ATCC (CRL-1730) and grown in a complete endothelial cell culture medium (IMC-309, Immocell Biotechnology). The cells were kept in a humidified incubator with 5% CO_2. For ox-LDL (L34357, Invitrogen) treatment, the cells were incubated with specified concentrations of ox-LDL for 48 hours. For SFI treatment, the cells were exposed to varying concentrations of PBS-diluted SFI for 24 hours. The SFI was acquired from China Resources Sanjiu Medical & Pharmaceutical, respectively.

shRNAs and non-viral transfection

The control and CLDN4-targeting shRNAs were respectively inserted into the PLKO.1-TRC-puro plasmid to create two resultant plasmids, called shNC and shCLDN4-1/-2/-3, respectively. The plasmids were further subjected to sequencing to ensure the accuracy of the inserted DNA fragments. The primers used for plasmid synthesis are provided in Table 1. The plasmid transfection was carried out using the ExFect transfection reagent (T101, Vazyme, China), following the directions provided by the manufacturer.

CCK-8 assay

At first, 2,000 HUVECs were seeded into each well of a 96-well plate, and the cells were grown overnight. The cells were then treated with specified concentrations of ox-LDL for 48 hours or SFI for 24 hours. For combined treatment, cells were exposed to both oxLDL and SFI for 48 hours. Following the treatment, 10 μL of CCK8 solution (ab228554, Abcam) was introduced into each well and left to incubate at a temperature of 37°C for a duration of 1.5 hours. The OD_{450} values were subsequently measured using a Flexstation3 microplate reader (Molecular Devices, USA).

Annexin V/PI assay

Annexin V/PI staining was used to evaluate cell apoptosis with the Apoptosis Detection Kit (V13242, Invitrogen). The specified treatments were applied to HUVECs after they were seeded into 6-well plates. After detaching and pelleting the cells, they were resuspended in staining buffer. The next step was to incubate the cells in the dark for 10 minutes with a mixture of 10 μL of Annexin V/PI. The cell suspension was analyzed using a 1300 NovoCyte flow cytometer (Agilent Technologies, USA), and the results were processed with NovoExpress® software 1.4.1 (Agilent Technologies).

qPCR

Total RNA was extracted using TRIzol reagent (1559 6026, Invitrogen, USA) and then reverse-transcribed with HiScript® II Q RT SuperMix (R223-01, Vazyme, China). Using SYBR Green Master Mix (Q111-02, Vazyme), qPCR tests were carried out on a QuantStudio 6 machine (Thermo Fisher Scientific, USA). The $2^{-\Delta\Delta Ct}$ method was used to quantify the relative expression levels of the target genes. Here are the primers that were used for qPCR:

CLDN4-qF:
5’-GGGGCAAGTGTACCAACTG-3’
CLDN4-qR:
5’-GACACCGGCACTATCACCA-3’
18S-qF:
5’-CGACGACCCATTCGAACGTCT-3’
18S-qR:

5'-CTCTCCGGAATCGAACCCTGA-3.

Western blot

HUVECs were extracted with RIPA buffer and protease inhibitors. Protein concentrations were measured with a BCA kit. Samples were heated, separated by SDS-PAGE, and transferred to PVDF membranes. Membranes were blocked, incubated with primary antibodies, washed, and then incubated with secondary antibodies. Signals were detected with ECL and imaged using ChemiDoc. Band intensities were analyzed with Image J and normalized to β-actin. Antibodies and dilutions are listed in Table 2.

Malondialdehyde (MDA), GSH/GSSG, superoxide dismutase (SOD), and nitric oxide (NO) levels evaluation

MDA, GSH/GSSG, SOD, and NO levels were measured using MDA Colorimetric Assay Kit (EEA015, Invitrogen), Glutathione Colorimetric Assay Kit (EIAG SHC, Invitrogen), SOD Colorimetric Activity Assay Kit (EIASODC, Invitrogen), and Nitric Oxide Assay Kit (EMSNO, Invitrogen), respectively. All assays were conducted in accordance with the manufacturer's guidelines.

ROS level detection

By using a ROS Fluorometric Assay Kit from Invitrogen (EEA019), ROS levels were measured in accordance with the manufacturer's instructions. Briefly, HUVECs subjected to the specified treatments were resuspended in serum-free culture medium and incubated with DCF-DA at 37°C for 20 minutes in the dark with intermittent inversion. The cells were then washed with serum-free medium to remove any free DCF-DA. Finally, the cells were resuspended in PBS and examined using flow cytometry.

Establishment of acute pancreatitis (AP) rat model

Twenty male Sprague-Dawley rats weighing 180 - 260 grams were obtained from Zhejiang Vital River Laboratory Animal Technology Co., Ltd. They were randomly divided into five groups of six rats each: Sham, AP, AP+SFI, AP+SFI+AAV - shNC, and AP+SFI+AAV - shCLDN4. The rats were housed in a 12 - hour light/dark cycle environment with unrestricted food and water for one week. Rats in AAV-infected groups received a daily 100 μL intraperitoneal AAV injection (vector genomes = 8×10^{11}) for ten consecutive days. Rats in SFI treatment groups were given a 10 mL/kg intraperitoneal SFI injection 30 minutes before surgery. All rats were fasted for 12 hours before surgery.

During the surgery, rats were anesthetized by 3% isoflurane inhalation. A midline laparotomy was done to open the abdominal cavity, and the bile and pancreatic duct was blocked at the hepatic hilum with a vascular clamp. Then, a 24-gauge catheter was used to intubate the duodenum. Sham rats were injected with sterile saline, while other groups slowly received 1 mL/kg of 5% sodium taurocholate into the bile and pancreatic duct. Three days post-surgery, the rats were euthanized, and blood and pancreatic tissue samples were collected. The serum was used for ELISA assays, and the pancreatic tissue was partitioned into two sections: one section was preserved with 4% paraformaldehyde for histological investigation, while the other section was frozen at -80°C for further qPCR and Western blot assays.

The shNC and shCLDN4 adeno-associated virus recombinant vector plasmids were purchased from Genomeditech (Shanghai) Co., Ltd. We dissolved the recombinant vector plasmid (Heper Vector plasmid: rep/cap Vector plasmid = 1:1:1) and Obio transfection reagent separately in 500 μL Opti - MEM medium, mixed them well, and let them stand for 5 minutes each. Then, we added the Obio transfection reagent dilution dropwise into the plasmid dilution, mixed it gently, and left it at room temperature for 20 minutes to form a stable transfection complex. We added the complex to cultured AAV - 293T cells. After 6 hours, we aspirated the medium, washed it with PBS, and added 10 ml of fresh complete medium. AAV virus particles were collected from infected AAV - 293T cells 72 hours after transfection. The virus was purified by iodixanol gradient centrifugation, the viral liquid was concentrated in ultrafiltration tubes, and finally, the viral titer was detected by qPCR assay.

All experiments were approved by the Institutional Ethics Committee of Zhejiang Provincial People's Hospital (approval no. 20240731014701534252) and adhered to protocols approved by the Animal Care and Use Committee of Zhejiang Provincial People's Hospital.

Immunohistochemistry (IHC)

The tissue sections were first dewaxed and rehydrated. After antigen retrieval, they were treated with 3% hydrogen peroxide, permeabilized with 0.2% Triton X - 100 in PBS, and blocked with 1% BSA. Then, they were incubated with a Ki-67 antibody (ab15580, Abcam, UK, 1:500) at 4°C overnight. After a PBST wash, the sections were exposed to HRP-conjugated goat anti-rabbit IgG (SA00001 - 2, Proteintech, China, 1:1,000) at room temperature for one hour. Next, they were washed again and treated with a DAB working solution (34002, Thermo Scientific). Subsequently, they were counterstained with hematoxylin and mounted. Finally, images were captured using an IX73 inverted microscope (OLYMPUS, Japan), and Ki-67+ cells were determined using Image - Pro Plus 6.0 software (Media Cybernetics, USA).

Enzyme-linked immunosorbent assay (ELISA)

The concentrations of TNF-α, IL-1β, and IL-18 were measured using ELISA kits following the instructions provided by the manufacturer. TNF-α was measured using ab236712 (Abcam), IL-1β was measured using ab255730 (Abcam), and IL-18 was measured using ab213909 (Abcam).

Table 1. Primers for plasmid construction.

Primer name	Primer sequence (5'-3')
shCLDN4-1-F	CCGGACATCATCCAAGACTTCTACACTCGAGTGTAGAAGTCTTGGATGATGTTTTTT
shCLDN4-1-R	AATTAAAAAACATCATCCAAGACTTCTACACTCGAGTGTAGAAGTCTTGGATGATGT
shCLDN4-2-F	CCGGGCAACATTGTCACCTCGCAGACTCGAGTCTGCGAGGTGACAATGTTGCTTTTT
shCLDN4-2-R	AATTAAAAAGCAACATTGTCACCTCGCAGACTCGAGTCTGCGAGGTGACAATGTTGC
shCLDN4-3-F	CCGGCGCCCTCGTCATCATCAGCATCTCGAGATGCTGATGATGACGAGGGCGTTTTT
shCLDN4-3-R	AATTAAAAACGCCCTCGTCATCATCAGCATCTCGAGATGCTGATGATGACGAGGGCG
shNC-F	CCGGTTCTCCGAACGTGTCACGTTTCTCGAGAAACGTGACACGTTCGGAGAATTTTT
shNC-R	AATTAAAAATTCTCCGAACGTGTCACGTTTCTCGAGAAACGTGACACGTTCGGAGAA

Table 2. Western blot antibody information.

Target/Antibody name	Species	Manufacture	Catalog #	Dilution
Bax	Mouse	Immunoway, China	YM3619	1:500
Bcl2		Proteintech, China	60178-1-Ig	
Claudin-4	Rabbit	Immunoway	YT0951	
C-Caspase 3		Proteintech	19677-1-AP	
NRF2			80593-1-RR	
HO-1			10701-1-AP	
β-actin			20536-1-AP	1:1,000
HRP-Anti-Mouse IgG	Goat		SA00001-1	1:10,000
HRP-Anti-Rabbit IgG			SA00001-2	

Statistical analysis

Statistical analyses and the creation of charts were conducted using GraphPad Prism software (version 8.0). Data are presented as mean ± standard deviation (SD). Each data point represents the value of one biological replicate or the mean value of a technical triplicate. Unpaired two-tailed Student's *t*-tests were utilized to assess statistical significance between two groups of data. For comparisons involving three or more groups, one-way analysis of variance (ANOVA) was applied. Statistical significance was considered as a p-value of less than 0.05. The Annexin V/PI staining and Western blot were each replicated at least three times in independent experiments. The other *in vitro* experiments also included technical triplicates.

RESULTS

SFI protects HUVECs from ox-LDL-induced damage

To validate the influence of SFI on endothelial cells under oxidative stress, we first exposed HUVECs to various concentrations of ox-LDL. After 48 hours of culture, we evaluated cell viability by employing a CCK-8 test. The results indicated that all ox-LDL-treated HUVECs showed reduced viability (Figure S1A). For subsequent analyses, we selected a concentration of 40 μg/mL of ox-LDL. Consistently, Annexin V/PI staining showed that ox-LDL significantly increased apoptosis in HUVECs (Figure S1B and C). Additionally, ox-LDL treatment markedly elevated ROS levels in HUVECs, as evidenced by DCF-DA staining (Figure S1D and E).

Next, we evaluated the impact of different dosages of SFI on HUVECs using a CCK-8 assay. The results revealed that 80 μL/mL of SFI began to reduce HUVEC viability (Figure S1F), and this concentration was used in subsequent experiments.

After these optimizations, we examined the effect of SFI on ox-LDL-induced HUVECs. The results of the Annexin V/PI staining data demonstrated that SFI treatment significantly inhibited apoptosis in HUVECs exposed to ox-LDL (Figure 1A and B). Consistent with this finding, SFI treatment improved the viability of ox-LDL-induced HUVECs (Figure 1C). Furthermore, SFI reduced the elevated ROS levels in HUVECs exposed to ox-LDL, as indicated by DCF-DA staining (Figure

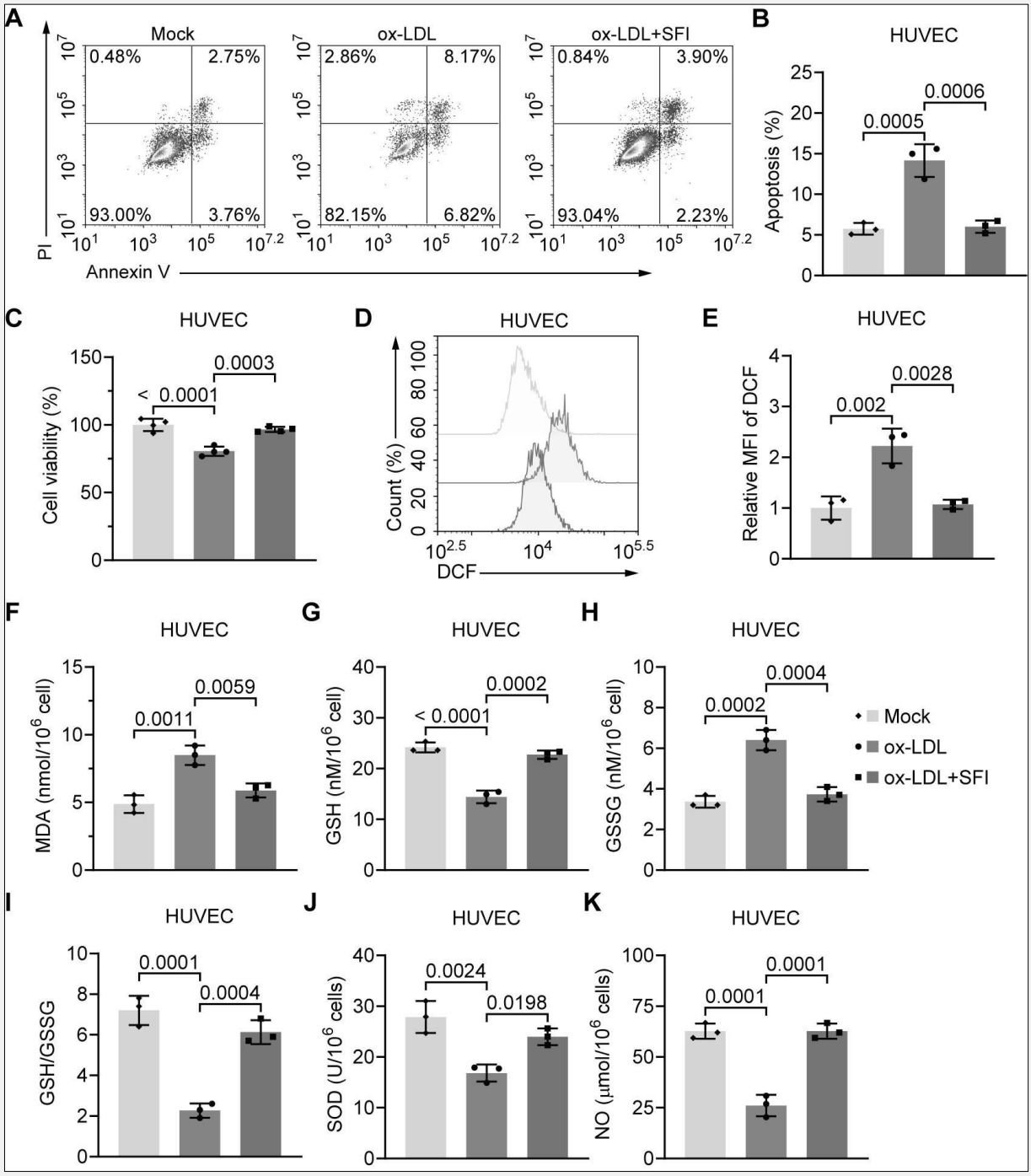

Figure 1. SFI protects HUVECs from ox-LDL-triggered injury. A, B - Annexin V/PI staining data showing the apoptosis of HUVECs with the specified treatments. C - CCK-8 assay results depicting the viability of cells with the specified treatments. D, E - DCF-DA staining outcomes indicating the ROS levels of HUVECs with the specified treatments. F - K - The levels of MDA (F), GSH (G), GSSG (H), GSH/GSSG (I), SOD (J), and NO (K) in HUVECs with the specified treatments.

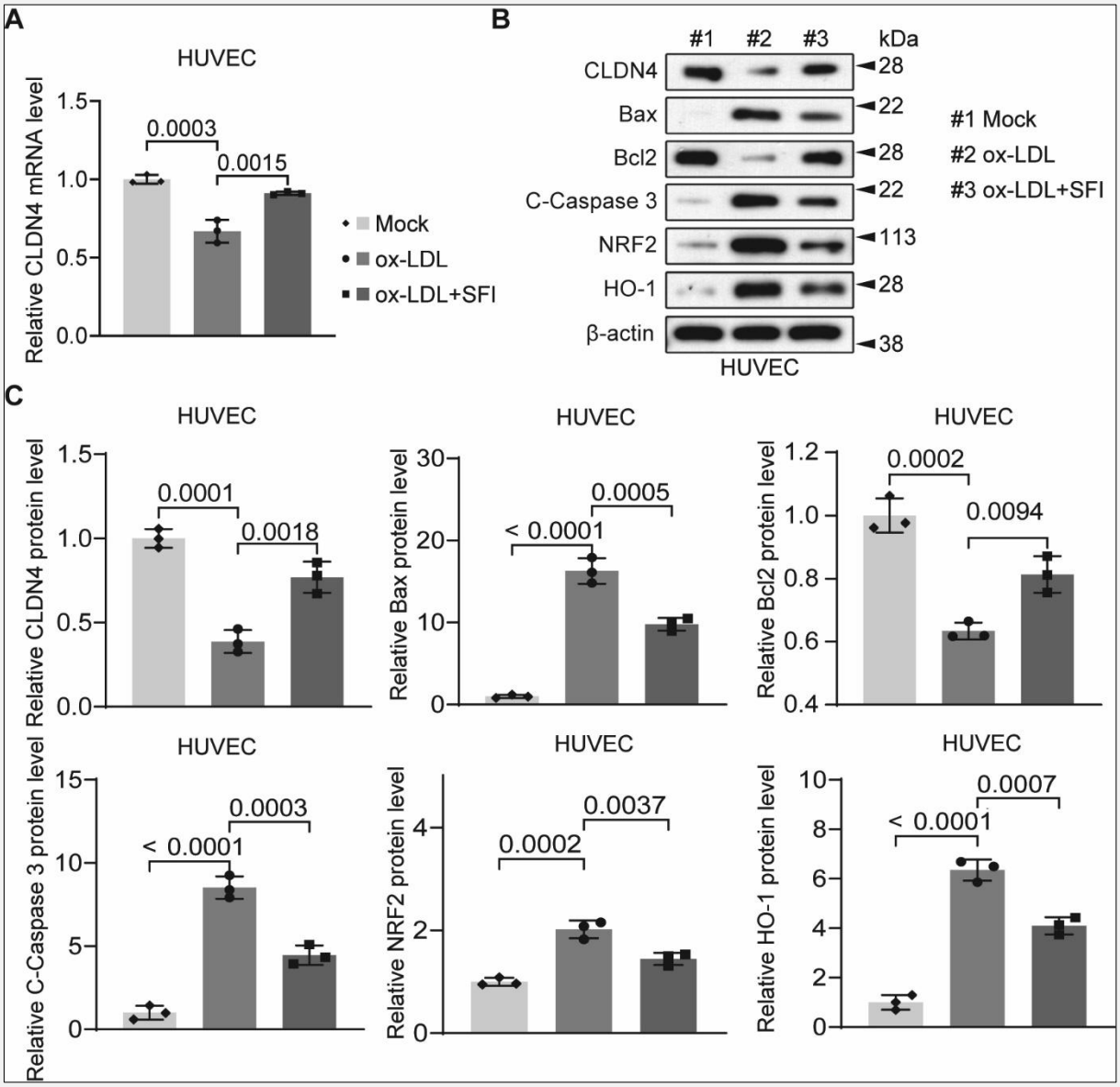

Figure 2. SFI affects the expression of CLDN4 and genes associated with apoptosis and ROS levels in ox-LDL-treated HUVECs. A - qPCR data showing the mRNA level of CLDN4 in cells with the specified treatments. B, C - Western blot results indicating the protein expression of CLDN4, Bax, Bcl2, C-Caspase 3, NRF2, and HO-1 in HUVECs with the specified treatments.

1D and E). This conclusion was further supported by SFI's ability to lower MDA and GSSH levels while increasing GSH and SOD levels in HUVECs exposed to ox-LDL (Figure 1F - J). Additionally, SFI treatment increased NO levels in HUVECs exposed to ox-LDL, indicating improved endothelial cell function (Figure 1K). Taken together, these observations demonstrate that SFI has a protective effect on HUVECs under oxidative stress.

SFI induces CLDN4 expression and represses genes controlling apoptosis and ROS levels in ox-LDL-treated HUVECs

In order to clarify the mechanism by which SFI protects HUVECs, we initially investigated the expression of CLDN4, a protein that is known to be increased in lung tissues by SFI [15]. qPCR data revealed that CLDN4 expression in HUVECs was suppressed by ox-LDL but was restored upon SFI exposure (Figure 2A). Consis-

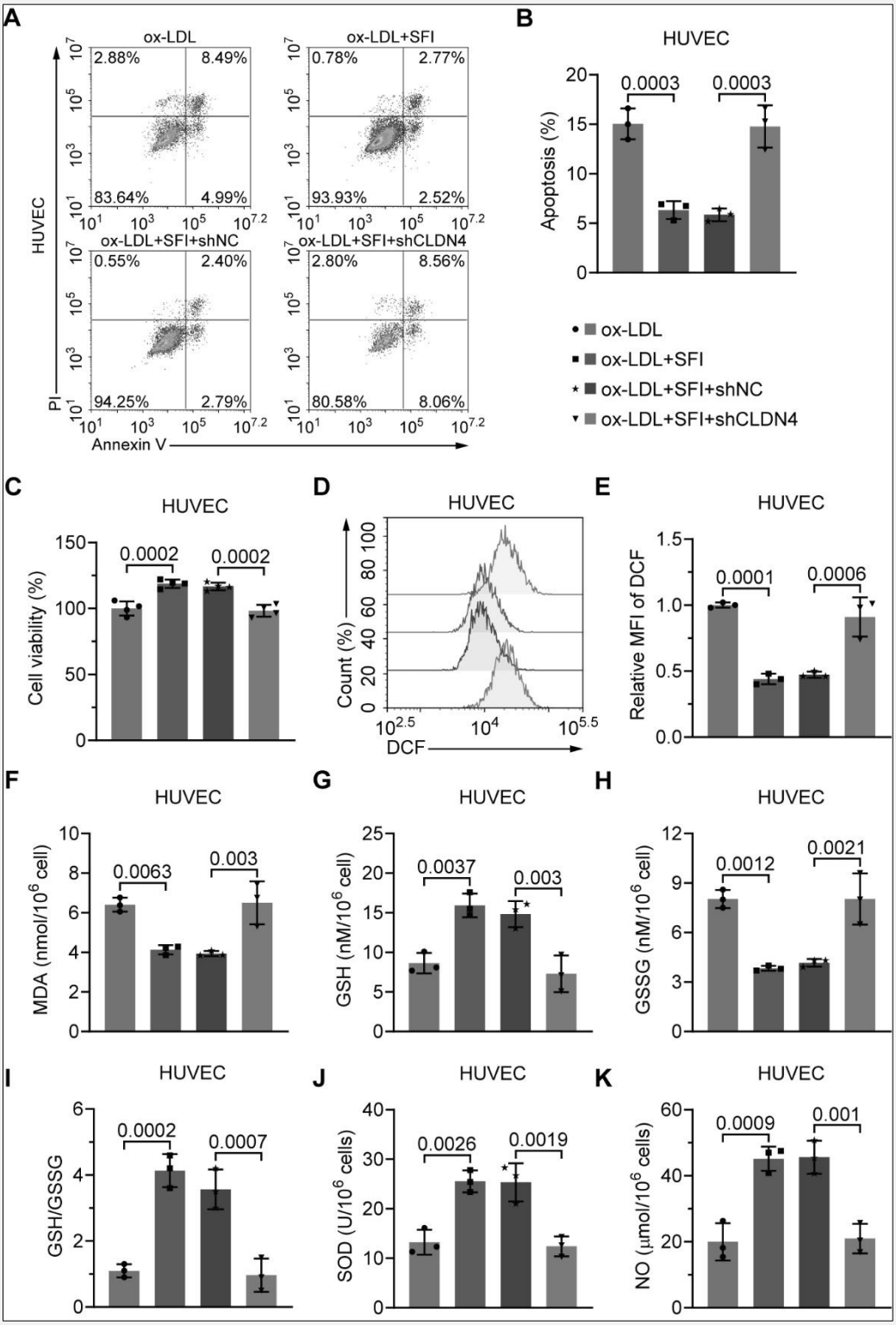

Figure 3. CLDN4 is required for SFI to exert its protective effect on HUVECs exposed to ox-LDL. A, B - Annexin V/PI staining data indicating the apoptosis of HUVECs with the specified treatments. C - CCK-8 assay results showing the viability of HUVECs with the specified treatments. D, E - DCF-DA staining outcomes revealing the ROS levels of HUVECs with the specified treatments. F - K - The levels of MDA (F), GSH (G), GSSG (H), GSH/GSSG (I), SOD (J), and NO (K) in HUVECs with the specified treatments.

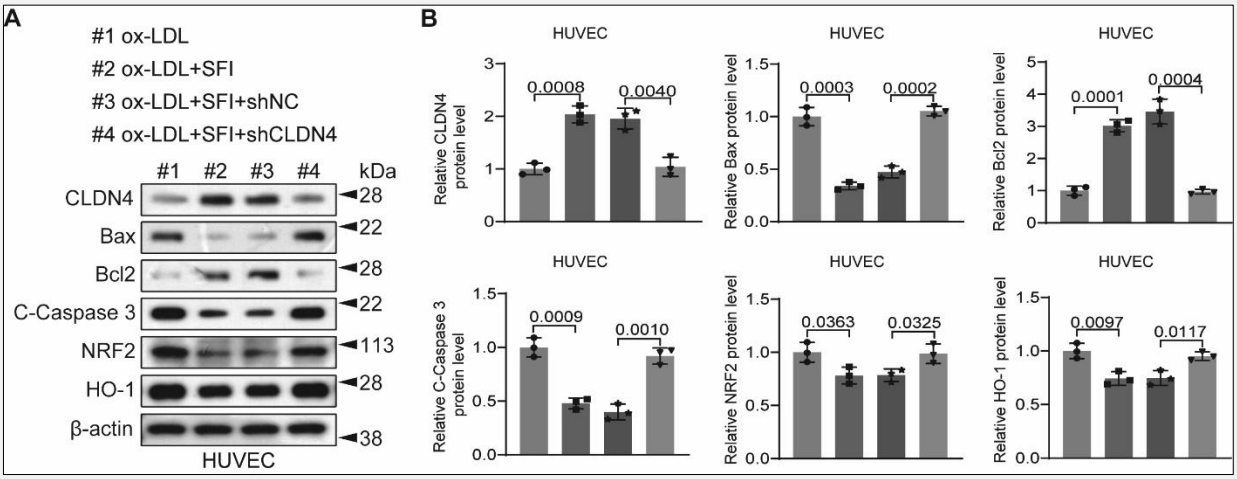

Figure 4. Depletion of CLDN4 disrupts the influence of SFI on the levels of genes linked to apoptosis and ROS levels in HUVECs exposed to ox-LDL. A, B - Western blot outcomes indicating the levels of CLDN4, Bax, Bcl2, C-Caspase 3, NRF2, and HO-1 in HUVECs with the specified treatments.

tently, Western blot data confirmed that SFI could rescue the reduced CLDN4 expression in HUVECs exposed to ox-LDL (Figure 2B and C). Given the anti-apoptotic role of CLDN4, we subsequently evaluated genes involved in apoptosis regulation. Western blot analysis showed that SFI decreased the levels of pro-apoptotic proteins BAX and C-Caspase 3, while increasing the level of the anti-apoptotic protein Bcl2 in HUVECs exposed to ox-LDL (Figure 2B and C). Additionally, the levels of NRF2 and HO-1, which are stimulated by oxidative stress [16,17], were significantly downregulated by SFI (Figure 2B and C). These results suggest that SFI reduces apoptosis and ROS levels in oxidative-stressed HUVECs, potentially by restoring CLDN4 expression.

Depletion of CLDN4 mitigates the protective effect of SFI on ox-LDL-treated HUVECs

To determine whether CLDN4 mediates the protective function of SFI in HUVECs under oxidative stress, we planned to knock down CLDN4 expression in these cells. We started by testing the knockdown efficiency of shRNAs targeting CLDN4. qPCR results showed that all three shCLDN4s were highly efficient in depleting CLDN4 in HUVECs (Figure S2A). Since shCLDN4-2 exhibited the highest efficiency, we used this shRNA in subsequent analyses. The data also confirmed that CLDN4 mRNA expression was significantly knocked down by this shCLDN4 in HUVECs exposed to ox-LDL and SFI (Figure S2B).

Following this, we assessed the effect of SFI on CLDN4-deficient HUVECs under oxidative stress. The data from Annexin V/PI staining indicated that CLDN4 reduction abolished the anti-apoptotic effect of SFI on these cells (Figure 3A and B). The CCK-8 assay results indicated that the pro-viability impact of SFI on these cells was nullified upon CLDN4 deficiency (Figure 3C). Furthermore, the antioxidant effect of SFI on ox-LDL-induced HUVECs was mitigated by CLDN4 depletion, as indicated by the levels of DCF-DA, MDA, GSH, GSSH, and SOD in these cells (Figure 3D-J). Additionally, SFI could no longer improve the function of CLDN4-deficient HUVECs exposed to ox-LDL, as their NO levels were comparable to those of control oxidative stressed HUVECs (Figure 3K).

At the molecular level, CLDN4 deficiency led to upregulated Bax, C-Caspase 3, NRF2, and HO-1 levels, and reduced expression of Bcl2 (Figure 4A and B). These Western blot data further supported the finding that the anti-apoptotic and antioxidant effects of SFI were mitigated in CLDN4-deficient HUVECs under ox-LDL treatment. Collectively, these findings indicate that CLDN4 plays a crucial role in SFI's protective effect on oxidative stressed HUVECs.

CLDN4 deficiency attenuates the impact of SFI on the pancreatic tissue of AP rats

To investigate whether the SFI-CLDN4 pathway mitigates pancreatic tissue damage caused by acute pancreatitis (AP) *in vivo*, we developed a rat model of AP. Histological examination using H&E staining revealed that AP rats exhibited significant loss of acinar cells, infiltration by immune cells, and formation of cyst-like structures (Figure 5A). Administration of SFI reduced

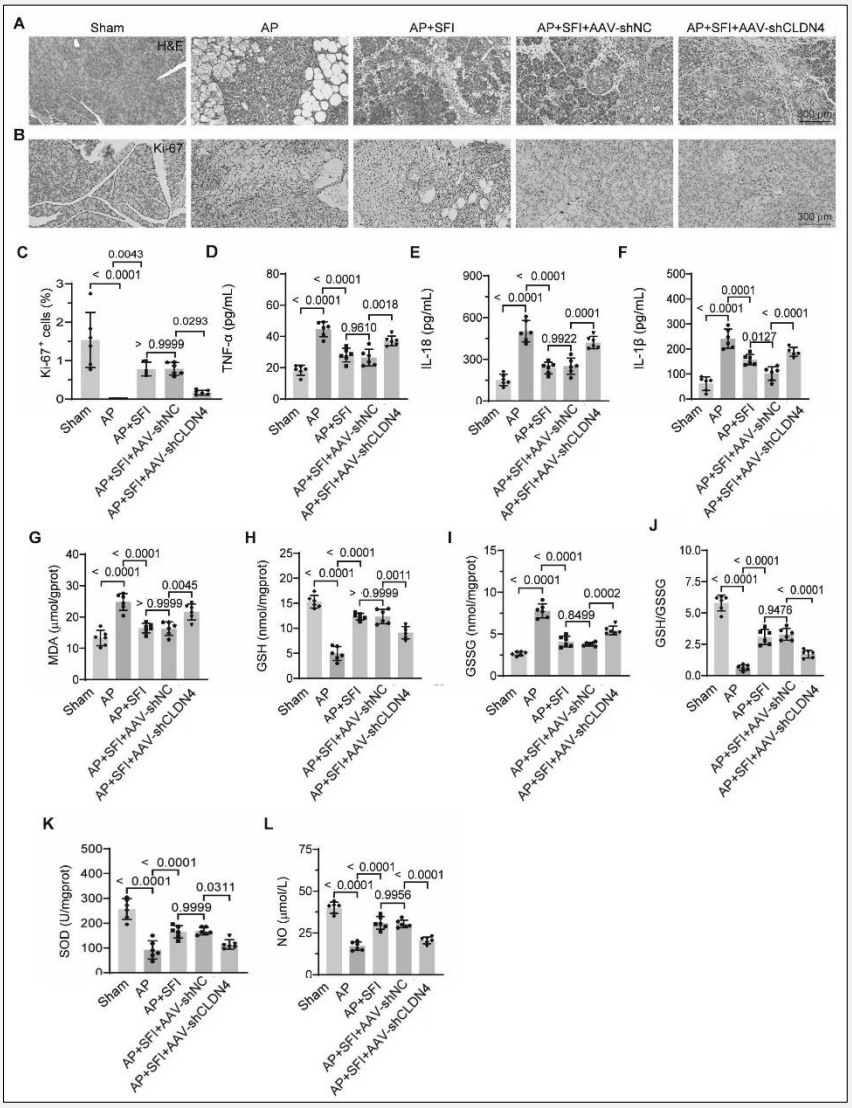

Figure 5. CLDN4 mediates the protective effect of SFI on the pancreatic tissues of AP rats. A - H&E staining data showing the structure of pancreatic tissue from rats with the specified treatments. B, C - IHC data indicating the Ki-67 expression in the pancreatic tissues of rats with the specified treatments. D - F - ELISA results illustrating the levels of circulating TNF-α (D), IL-18 (E), and IL-1β (F) in rats with the specified treatments. G - L - The levels of MDA (G), GSH (H), GSSG (I), GSH/GSSG (J), SOD (K), and NO (L) in the pancreatic tissues from rats with the specified treatments.

the loss of pancreatic acinar cells; however, this protective effect was diminished when AAVs carrying shCLDN4 were introduced (Figure 5A). Consistent with this, Ki-67 staining showed that SFI partially restored acinar cell proliferation, but this benefit was less pronounced with AAV-shCLDN4 administration (Figure 5B and C). Additionally, elevated levels of IL-1β, IL-18, and TNF-α in AP rats were significantly decreased by SFI, though the reduction was less evident with AAV-shCLDN4 infection (Figure 5D - F). SFI also impacted the levels of MDA, GSH, GSSG, SOD, and NO in the pancreatic tissues of AP rats, but this effect was diminished in the presence of AAV-shCLDN4 (Figure 5G - L).

Molecularly, Western blot analyses confirmed a decrease in CLDN4 expression in the pancreatic tissue of AP rats. SFI treatment effectively restored CLDN4 levels, but this restoration was significantly reduced in the presence of AAV-shCLDN4. Additionally, Western blotting revealed that AP rats had increased levels of

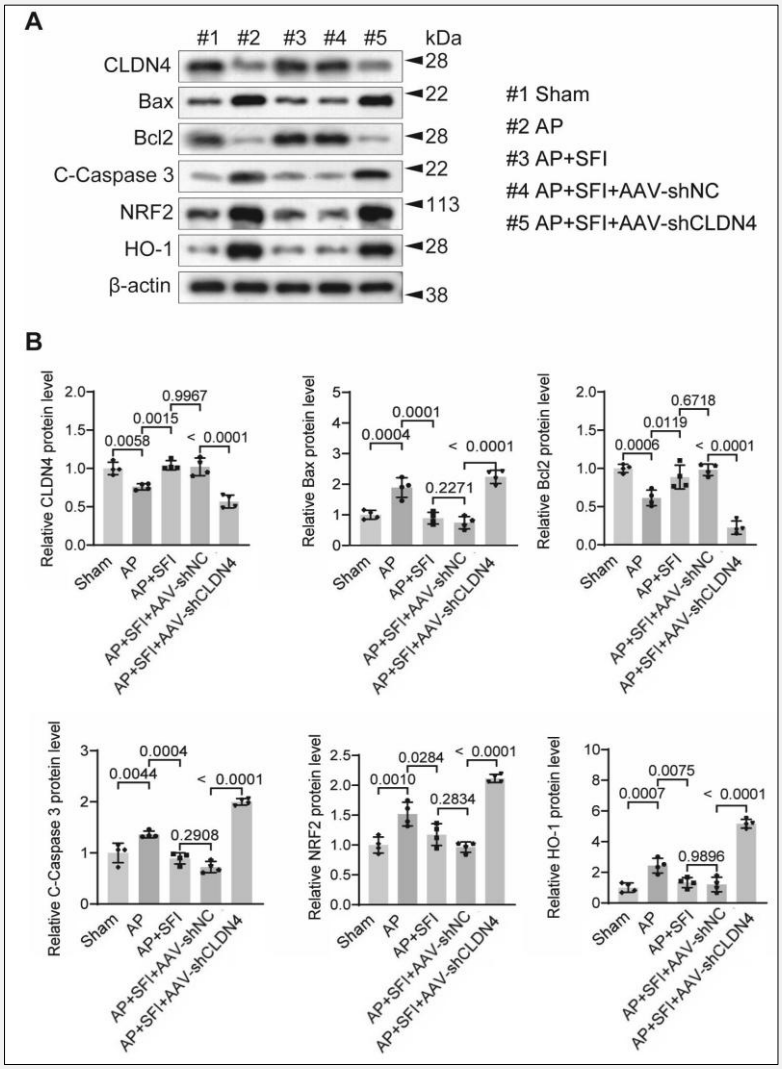

Figure 6. CLDN4 deficiency abolishes the influence of SFI on the expression of genes correlated with apoptosis and ROS levels in the pancreatic tissues of AP rats. A, B - Western blot results showing the levels of CLDN4, Bax, Bcl2, C-Caspase 3, NRF2, and HO-1 in the pancreatic tissues of rats with the specified treatments.

Bax, C-Caspase 3, NRF2, and HO-1, alongside a decreased Bcl2 level. SFI treatment reversed these alterations, but this protective effect was lost when CLDN4 was deficient (Figure 6A and B). The results suggest that CLDN4 is essential to the protective effects of SFI on pancreatic tissues damaged by AP.

DISCUSSION

TCM exhibits significant potential in treating various diseases. However, its clinical application is frequently constrained by the unclear nature of its active components and the absence of well-defined pharmacological mechanisms. This study investigated the pharmacological mechanism of SFI, a TCM renowned for addressing conditions involving endothelial dysfunction.

SFI's protective effects on the cardiovascular system have been extensively documented through animal models and clinical trials [18-23]. The data align with these findings, demonstrating that SFI reduces apoptosis, enhances cell viability, and lowers ROS levels in HUVECs under oxidative stress. Excessive ROS levels are commonly linked to endothelial dysfunction, as ROS can directly damage endothelial cells [24], suggesting that SFI's antioxidant properties may signifi-

cantly contribute to its protective effects. Nevertheless, the precise molecular process remains unclear.

For instance, promoter hypermethylation or hypomethylation has been associated with decreased or elevated CLDN4 expression in various cancers [28-30]. Secreted signaling molecules, such as TGF-β and HIF1α, also modulate CLDN4 expression in diverse contexts [31, 32]. Additionally, inflammation can influence CLDN4 expression through inflammatory cytokines like TNF-α and IL-18 in other scenarios [33,34]. In HUVECs, treatment with ox-LDL suppresses CLDN4 expression, indicating that oxidative stress serves as another regulator of CLDN4 via an uncharacterized mechanism. Conversely, the precise mechanism by which SFI restores CLDN4 expression in these cells remains elusive.

In inflammatory pancreatic tissues, CLDN4 expression is similarly downregulated, potentially due to heightened cytokine levels. SFI not only rescues CLDN4 expression but also reduces circulating cytokine levels, hinting at a possible feedback loop between CLDN4 and inflammation. Further research is warranted to investigate these hypotheses.

The study offers evidence that the SFI-CLDN4 axis mitigates pancreatic tissue damage in AP rats. Although this effect is primarily attributed to the amelioration of endothelial dysfunction, it is also plausible that the SFI-CLDN4 axis directly influences other cell types, such as pancreatic acinar cells, by enhancing their proliferation, survival, and function, akin to its effects observed in inflammatory lung tissue [15]. Further detailed analyses are necessary to pinpoint the exact targets of the SFI-CLDN4 axis within inflammatory pancreatic tissue.

CONCLUSION

In summary, the data underscore the crucial role of CLDN4 in mediating the protective effects of SFI on oxidative-stressed HUVECs and inflammatory pancreatic tissues. This study deepens our understanding of SFI's pharmacological mechanisms and the functional significance of CLDN4, thereby highlighting the therapeutic potential of targeting the SFI-CLDN4 axis for treating conditions characterized by endothelial dysfunction, such as acute pancreatitis (AP).

Source of Funds:
This work was supported by the Zhejiang Province Medical and Health Science and Technology Plan Project (2023KY016) and Zhejiang Province Traditional Chinese Medicine Science and Technology Plan Project (2023ZL245).

Ethical Approval Statement:
The study was approved by the Institutional Ethics Committee of Zhejiang Provincial People's Hospital (approval no. 20240731014701534252) and adhered to protocols approved by the Animal Care and Use Committee of Zhejiang Provincial People's Hospital.

Data Availability Statement:
All data supporting the conclusion of this study have been included in the manuscript and the supplemental files and are available from the corresponding author upon reasonable request.

Declaration of Interest:
The authors declare that they have no conflicts of interest to declare.

References:

1. Mederos MA, Reber HA, Girgis MD. Acute Pancreatitis: A Review. JAMA 2021;325(4):382-90. (PMID: 33496779)
2. Weiss FU, Laemmerhirt F, Lerch MM. Etiology and Risk Factors of Acute and Chronic Pancreatitis. Visc Med 2019;35(2):73-81. (PMID: 31192240)
3. Zheng Z, Ding Y-X, Qu Y-X, Cao F, Li F. A narrative review of acute pancreatitis and its diagnosis, pathogenetic mechanism, and management. Ann Transl Med 2021;9(1):69. (PMID: 33553362)
4. Singh VK, Wu BU, Bollen TL, et al. Early Systemic Inflammatory Response Syndrome Is Associated With Severe Acute Pancreatitis. Clin Gastroenterol Hepatol 2009;7(11):1247-51. (PMID: 19686869)
5. Komara NL, Paragomi P, Greer PJ, et al. Severe acute pancreatitis: capillary permeability model linking systemic inflammation to multiorgan failure. Am J Physiol Gastrointest Liver Physiol 2020;319(5):G573-83. (PMID: 32877220)
6. Trimm E, Red-Horse K. Vascular endothelial cell development and diversity. Nat Rev Cardiol 2023;20(3):197-210. (PMID: 36198871)
7. Krüger-Genge A, Blocki A, Franke R-P, Jung F. Vascular Endothelial Cell Biology: An Update. Int J Mol Sci 2019;20(18):4411. (PMID: 31500313)
8. Little PJ, Askew CD, Xu S, Kamato D. Endothelial Dysfunction and Cardiovascular Disease: History and Analysis of the Clinical Utility of the Relationship. Biomedicines 2021;9(6):699. PMID: 34203043)
9. Takeda Y, Matoba K, Sekiguchi K, et al. Endothelial Dysfunction in Diabetes. Biomedicines 2020;8(7):182. (PMID: 32610588)
10. Wang X, Guo Y, Cui T, et al. Telomerase reverse transcriptase restores pancreatic microcirculation profiles and attenuates endothelial dysfunction by inhibiting mitochondrial superoxide production: A potential target for acute pancreatitis therapy. Biomed Pharmacother 2023;167:115576. (PMID: 37776643)
11. Song Y, Zhang N, Shi S, et al. Large-scale qualitative and quantitative characterization of components in Shenfu injection by integrating hydrophilic interaction chromatography, reversed phase liquid chromatography, and tandem mass spectrometry. J Chromatogr A 2015;1407:106-18. (PMID: 26143607)
12. Xu F-F, Xie X-F, Hu H-Y, Tong R-S, Peng C. Shenfu injection: a review of pharmacological effects on cardiovascular diseases. Front Pharmacol 2024;15:1279584. (PMID: 38420190)

13. Huang L, Cao J. The protective effects of Shen-Fu injection on experimental acute pancreatitis in a rat model. Oxid Med Cell Longev 2014;2014:248786. (PMID: 24738018)

14. Zhu J, Song W, Xu S, et al. Shenfu Injection Promotes Vasodilation by Enhancing eNOS Activity Through the PI3K/Akt Signaling Pathway *In Vitro*. Front Pharmacol 2020;11:121. (PMID: 32161546)

15. Zheng Y, Zheng M, Shao J, et al. Upregulation of claudin-4 by Chinese traditional medicine Shenfu attenuates lung tissue damage by acute lung injury aggravated by acute gastrointestinal injury. Pharm Biol 2022;60(1):1981-93. (PMID: 36226770)

16. Ngo V, Duennwald ML. Nrf2 and Oxidative Stress: A General Overview of Mechanisms and Implications in Human Disease. Antioxidants (Basel) 2022;11(12):2345. (PMID: 36552553)

17. Chiang S-K, Chen S-E, Chang L-C. The Role of HO-1 and Its Crosstalk with Oxidative Stress in Cancer Cell Survival. Cells 2021;10(9):2401. (PMID: 34572050)

18. Fan K-L, Wang J-H, Kong L, et al. Effect of Shen-Fu Injection on Hemodynamics in Early Volume Resuscitation Treated Septic Shock Patients. Chin J Integr Med 2019;25(1):59-63. (PMID: 28986814)

19. Liao J, Qin C, Wang Z, et al. Effect of shenfu injection in patients with septic shock: A systemic review and meta-analysis for randomized clinical trials. J Ethnopharmacol 2024;320:117431. (PMID: 37981120)

20. Wang S, Liu G, Chen L, et al. Effects of shenfu injection on sublingual microcirculation in septic shock patients: A randomized controlled trial. Shock 2022;58(3):196-203. (PMID: 35959775)

21. Hua T, Lu Z, Wang M, et al. Shenfu injection alleviate gut ischemia/reperfusion injury after severe hemorrhagic shock through improving intestinal microcirculation in rats. Heliyon 2024; 10(11):e31377. (PMID: 38845930)

22. Zhang M-Q, Zhang Q, Yuan W, et al. Protective Effect of Shenfu Injection on Vascular Endothelial Damage in a Porcine Model of Hemorrhagic Shock. Chin J Integr Med 2022;28(9):794-801. (PMID: 35023060)

23. Gu W, Li C, Yin W, Guo Z, Hou X, Zhang D. Shen-Fu Injection Reduces Postresuscitation Myocardial Dysfunction in a Porcine Model of Cardiac Arrest by Modulating Apoptosis. Shock 2012; 38(3):301-6. (PMID: 22683733)

24. Incalza MA, D'Oria R, Natalicchio A, Perrini S, Laviola L, Giorgino F. Oxidative stress and reactive oxygen species in endothelial dysfunction associated with cardiovascular and metabolic diseases. Vascul Pharmacol 2018;100:1-19. (PMID: 28579545)

25. Günzel D, Yu ASL. Claudins and the modulation of tight junction permeability. Physiol Rev 2013;93(2):525-69. (PMID: 23589827)

26. Fujiwara-Tani R, Mori S, Ogata R, et al. Claudin-4: A New Molecular Target for Epithelial Cancer Therapy. Int J Mol Sci 2023; 24(6):5494. (PMID: 36982569)

27. Breed C, Hicks DA, Webb PG, et al. Ovarian Tumor Cell Expression of Claudin-4 Reduces Apoptotic Response to Paclitaxel. Mol Cancer Res 2019;17(3):741-50. (PMID: 30606772)

28. Kwon MJ, Kim S-S, Choi Y-L, et al. Derepression of CLDN3 and CLDN4 during ovarian tumorigenesis is associated with loss of repressive histone modifications. Carcinogenesis 2010;31(6): 974-83. (PMID: 20053926)

29. Boireau S, Buchert M, Samuel MS, et al. DNA-methylation-dependent alterations of claudin-4 expression in human bladder carcinoma. Carcinogenesis 2007;28(2):246-58. (PMID: 16829686)

30. Maesaka F, Kuwada M, Horii S, et al. Hypomethylation of CLDN4 Gene Promoter Is Associated with Malignant Phenotype in Urinary Bladder Cancer. Int J Mol Sci 2022;23(12):6516. (PMID: 35742959)

31. Rachakonda G, Vu T, Jin L, Samanta D, Datta PK. Role of TGF-β-induced Claudin-4 expression through c-Jun signaling in non-small cell lung cancer. Cell Signal 2016;28(10):1537-44. (PMID: 27424491)

32. Liu H, Zhang Z, Zhou S, et al. Claudin-1/4 as directly target gene of HIF-1α can feedback regulating HIF-1α by PI3K-AKT-mTOR and impact the proliferation of esophageal squamous cell though Rho GTPase and p-JNK pathway. Cancer Gene Ther 2022;29(6): 665-82. (PMID: 34276052)

33. Fujiwara-Tani R, Sasaki T, Luo Y, et al. Anti-claudin-4 extracellular domain antibody enhances the antitumoral effects of chemotherapeutic and antibody drugs in colorectal cancer. Oncotarget 2018;9(100):37367-78. (PMID: 30647838)

34. Yang Y, Cheon S, Jung MK, et al. Interleukin-18 enhances breast cancer cell migration via down-regulation of claudin-12 and induction of the p38 MAPK pathway. Biochem Biophys Res Commun 2015;459(3):379-86. (PMID: 25727011)

Additional material can be found online at:
http://supplementary.clin-lab-publications.com/250673/